SAND2009-7653C

CORRELATING PETN COOKOFF VIOLENCE WITH PRE-IGNITION DAMAGE [*]

M.L. Hobbs, W.B. Wente, and M.J. Kaneshige
Sandia National Laboratories[†]
Albuquerque, NM

ABSTRACT

A pentaerythritol tetranitrate (PETN) ignition model has been developed using data from various sources. The one-step, first-order, *pressure-independent* mechanism was used to predict pressure, temperature, and time to ignition for various small-scale experiments. Liquid reaction rates were assumed to be four times (4×) larger than solid reaction rates. Simultaneous decomposition with melting produced a two-phase frothy material with a gas-like thermal conductivity. The uncertainties in melting point and reaction rates were correlated to uncertainty in ignition times. The PETN thermal response model was validated using time to ignition, pressure, and temperature data. The PETN model does not predict cookoff violence. However, the model can be used to assess the state of the degraded PETN at the onset of ignition. We propose that cookoff violence can be correlated with the extent of reaction at the onset of ignition. This hypothesis is tested using cookoff data from detonators encased in copper. We also tested the hypothesis by comparing post-ignition photos of Sandia's instrumented thermal ignition (SITI) experiment. The onset of ignition is determined using a storage Damköhler number, which is similar to a Damköhler (group IV) number, $D_a IV$.

INTRODUCTION

Predicting the response of PETN during an accident, such as a fire, is important for high consequence safety analysis. The response depends on many factors such as the thermophysical properties of PETN as well as temperature sensitive decomposition kinetics. Knowledge of properties associated with solid, liquid, and frothy PETN is necessary to predict and mitigate inadvertent thermal ignition. Some of these properties have been measured in Sandia's instrumented thermal ignition (SITI) experiment [1] and Lawrence Livermore's one-dimensional time-to-explosion (ODTX) experiment [2]. The present work increases our understanding of complex pre-ignition reactions and thermophysical changes in PETN leading to thermal runaway. An overview of thermal runaway leading to ignition can be found elsewhere [3-5]. Post ignition burning and resulting violence is beyond the scope of the current memo. However an empirical method to assess the potential for cookoff violence, such as reported by Zucker et al. [6] for PETN filled detonators, is discussed.

The current work uses ignition time, temperature, and pressure to construct the decomposition model. Mass loss and gas molecular weight are inferred assuming chemical equilibrium. Experiments are needed to quantify mass loss and gas molecular weight. The remainder of this paper describes various experiments used to characterize PETN. A simple model is formulated based on a single step reaction mechanism with the products assumed to be in equilibrium. The thermophysical properties as well as the decomposition rates were inferred from SITI and ODTX experiments. The model was applied to detonators containing PETN at various heating rates to evaluate detonator failure during cookoff. The model was also used to evaluate post-ignition photos of the SITI experiments.

---

[*] Approved for public release; distribution is unlimited.

[†] Sandia is a multiprogram laboratory operated by Sandia Corporation, a Lockheed Martin Company, for the United States Department of Energy's National Nuclear Security Administration under Contract DE-AC04-94AL85000.

MODEL

Hobbs et al. [7] have modeled ignition of PETN using a one-step, *pressure independent* reaction mechanism based on chemical equilibrium using the JCZS-EOS [8].* Figure 1 shows the mass fraction based reaction with 2.5 mass percent of the equilibrium products being carbon (*C* in Figure 1). The molecular weight of the gaseous equilibrium products was 30.8 g/mol and the reaction enthalpy was 6.45×10^6 J/kg of PETN.

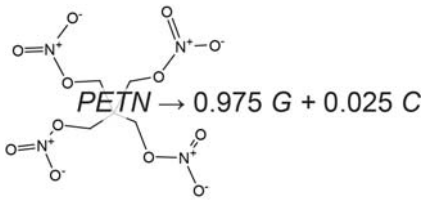

Figure 1. Mass fraction based reaction.

Thermal ignition of PETN was determined by solving the single temperature equations, $T_c = T_g = T(x,y,z,t)$, given in Tables 1 and 2 with the finite element code Calore [9]. Pressure was assumed to be only a function of time, changing with temperature and reaction. Radiation enclosures were included with equations and solution techniques described in reference [9]. Free convective energy exchange in enclosures was determined with equation 3 in Table 1 with the convection coefficient (h) set to 1 W/m^{2}K. The PETN material parameters and experiment specific parameters are given in Table 3 and 4, respectively. The boundary and initial temperatures were specified. Solution of these equations provided the time-resolved temperature and species concentrations within the decomposing PETN and the temperature of the inert materials that confine the PETN. Typical properties are used for inert materials such as aluminum and copper.

The transition from solid to liquid thermal conductivity was modeled with a smooth hyperbolic tangent with the same transition width as the phase change width as shown in footnote "c" of Table 3. This same transition function was used to increase the liquid reaction rates to be four times faster than the solid reaction rates, *e.g.* $\xi = 4$. Manelis et al. [10] postulated that PETN decomposition rates in the liquid can be 100-360 times greater than in the solid. But, predicted ignition times with ξ set to 100 did not match *both* SITI and ODTX data, whereas predictions with ξ set to 4 did match both sets of data. Thus, the reactions in the liquid phase are assumed to be four times faster than in the solid phase, at least with the mechanism in the current article.

Flow of liquid PETN was assumed to be negligible since most of the PETN was solid at ignition. However, the partially melted PETN contains bubbles filled with decomposition gases. The thermal conductivity of this melt phase approaches the thermal conductivity of the decomposition gases. Low thermal conductivity of the melt phase enables the model to match ignition data for fast cookoff where boundary temperatures are high. Additional details of the PETN ignition model can be found in reference [7].

The density of liquid PETN has not been measured and is assumed to be the same as the solid density corrected for thermal expansion. The latent enthalpy is partitioned from 406 to 424 K using an effective capacitance method derived from 12 differential scanning calorimeter (DSC) tests as discussed in reference [7]. The specific heat is assumed to be linearly dependent on temperature using the two bulk specific heat values given in Table 3. The specific heat is increased to the effective capacitance values (C_{eff}) in Figure 2 when the temperature is in the range, 133°C (406 K) < T < 152°C (425 K), to account for latent effects.

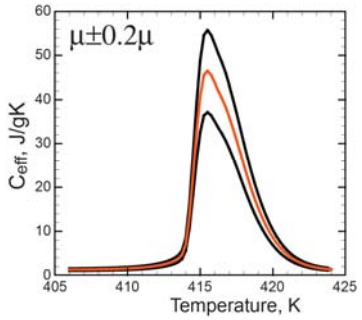

Figure 2. Effective thermal capacitance [7].

* This assumption does not imply that PETN decomposition is pressure independent. Rather, the model matches available data without using a pressure dependency. Few unsealed vented experiments have been performed. More experiments with controlled pressure are needed to characterize the effects of confinement and pressure.

Table 1. PETN ignition model showing domain[a]

Gas continuity (integral)	$\frac{dM_g}{dt} = \int_\Lambda r\rho_c^o\left(1-\phi^o\right)d\Lambda + \dot{m}_i - \dot{m}_o$	(1)
Gas momentum (low Mach)	$P(x,y,z,t) = P(t) = M_g / \int_\Lambda \frac{M_{wg}}{RT} d\Lambda$	(2)
Energy (integral: bulk elements)	$\frac{dV_b\rho_g C_g T_b}{dt} = -\int_S h\left(T_b - T\right)dS + \dot{m}_i h_i - \dot{m}_o h_o$	(3)
Energy (field: material blocks)	$\rho_b C_b \frac{\partial T}{\partial t} = \nabla\cdot(k\nabla T) + \rho_b h_r r$	(4)

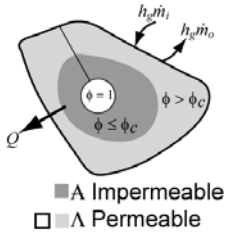

[a] C_b, C_g, h_i, h_o, h_r, k, $\dot{m}_i$, $\dot{m}_o$, M_g, M_{wg}, P, Q, r, ρ_c^o, R, S, t, T, T_b, V, x, y, z, ρ_b, ρ_g, ϕ, ϕ_c, ϕ^o and Λ represent bulk specific heat, gas specific heat, influx enthalpy, outflux enthalpy, reaction enthalpy, thermal conductivity, influx mass, outflux mass, mass of gas, molecular weight of gas, pressure, heat loss, reaction rate, initial density of condensed phase, gas constant, enclosure surface, time, temperature, bulk element temperature, volume, x-coordinate, y-coordinate, z-coordinate, bulk density, gas density, gas volume fraction, critical gas volume fraction, initial gas volume fraction, and permeable region, respectively.

Table 2. PETN reaction mechanism and auxiliary equations[b]

Mechanism	mole basis: $C_5H_8N_4O_{12} \rightarrow 4.17\ CO_2 + 2\ N_2 + 3.66\ H_2O + 0.17\ CH_4 + 0.66\ C$ or	
	mass basis: $petn \rightarrow 0.975\ gas + 0.025\ carbon$	(5)
Reaction Rate	$r = \frac{d}{dt}(petn) = \xi A\exp\left[-\left(E + z\sigma_E\right)/RT\right]petn$, where $petn(t=0) = 1$	(6)
Distribution parameter	$1 - petn = \int_{-\infty}^{z} \frac{1}{\sqrt{2\pi}}\exp\left(\frac{-z^2}{2}\right)dz$ or z = norminv$(1-petn)$	(7)
Gas volume fraction	$\phi = 1 - \left[S_f\left(1-\phi^o\right)\rho_c^o/\rho_c\right]$ where $S_f = petn + carbon$	(8)
Bulk density	$\rho_b = \phi\rho_g + (1-\phi)\rho_c$	(9)
Thermal conductivity	$k = \phi k_g + \frac{2}{3}(1-\phi)k_c + \frac{16\sigma T^3}{3\left[\phi\alpha_g + (1-\phi)\alpha_c\right]}$	(10)

[b] A, *carbon*, E, *gas*, k, k_c, k_g, **norminv**, *petn*, P, P^o, r, R, T, z, α_c, α_g, ϕ, ϕ^o, π, ρ_c, ρ_c^o, ρ_b, ρ_g, σ, σ_E, and ξ represent prefactor, carbon mass fraction, activation energy, gas mass fraction, effective thermal conductivity, condensed conductivity, gas conductivity, inverse of the normal probability distribution function, PETN mass fraction, pressure, initial pressure, reaction rate, gas constant, temperature, cumulative distribution parameter, condensed absorption, gas absorption, gas volume fraction, initial gas volume fraction, pi, condensed density, initial condensed density, bulk density, gas density, Stefan Boltzmann constant, activation energy dispersion, and liquid rate multiplier, respectively. Upper and lower bounds on *z* are 3.5 and -3.5.

Table 3. PETN material parameters

Parameter	description	value
α_c, m^{-1}	condensed absorption coefficient [11]	50000±10%
α_g, m^{-1}	gas absorption coefficient [12]	100±10%
β	volumetric expansion coefficient [13]	22.05×10^{-5}
C_{298}, C_{623} J/kgK	bulk specific heat at 298, 623 K [2]	1090, 1760[a]
E, J/kgmol	activation energy [14]	1.5×10^{8}
h_{pc}, J/kg	latent enthalpy (see Fig. 2)	1.77×10^{5} (implemented as C_{eff}±20%)
h_r, J/kg	reaction enthalpy[b]	6.45×10^{6}
k_c, W/mK	condensed thermal conductivity	$k_{fac}[\delta\times k_L + (1 - \delta)k_s]$[c]
$k_{g,300}$, $k_{g,500}$ W/mK	gas (air) conductivity at 300, 500 K [15]	0.0263, 0.0407[d]
k_L, W/mK	liquid conductivity to match fast cookoff	0.035±50%
k_{rate}	reaction rate uncertainty multiplier	1±10%
k_s, W/mK	solid conductivity to match SITI data	0.35±10%
$\mathrm{Ln}A$, $\mathrm{Ln}(s^{-1})$	natural logarithm of A	39.0
M_{wg}, g/mol	average gas molecular weight	30.8
M_{wgo}, g/mol	initial gas (air) molecular weight	28
ρ_c, kg/m^3	condensed PETN density	$\rho_{co}/[1+\beta(T-T_o)]$
ρ_{co}, kg/m^3	initial solid PETN density	1780
σ_E/R, K	normalized activation energy dispersion	1260
T_{pc}, K	melting point (DSC data, see Fig 2.B)	415±1%
w_{pc}, K	melting point range	2±10%
ξ	liquid rate multiplier (see Fig 2.B)	4.0±10% [implemented as $\xi = \delta + (1-\delta)4$]

[a]bulk heat capacity varies linearly between 298-623 K with constant extrapolation.
[b]based on equilibrium reaction: $C_5H_8N_4O_{12} \rightarrow 4.17\ CO_2 + 2\ N_2 + 3.66\ H_2O + 0.17\ CH_4 + 0.66\ C$.
[c]$\delta = 0.5\times\{1+\tanh[(T-T_{pc})/w_{pc}]\}$ for the transition.
[d]gas thermal conductivity varies linearly between 300-500 K with linear extrapolation.

Table 4. PETN experiment parameters [a]

parameter	description	ODTX[b]	SITI-powder [c]	SITI-pressed[d]	Detonator [e]
h, W/m^2K	convection coefficient	0	1	1	1
ρ_{bo}, kg/m^3	initial bulk density	1720±10	1101	1690±10	670
V_{enc}, cm^3	enclosure volume	0	7.05	1.51	0.713
V_{petn}, cm^3	bulk PETN volume	1.07	7.05	12.9	0.709
V_{tube}, cm^3	pressure tubing volume	0	0.2	0.2	0

[a]ODTX, SITI, and detonator are described in subsequent sections.
[b]half inch spheres exposed to constant temperature.
[c]test #102 vented since PETN crystals on the transducer threads were a safety concern. Outside temperature ramped to 418 K in 550 seconds, and then ramped at 1°C/minute until ignition at 1546 seconds.
[d]one inch diameter by one inch tall cylinders with the boundary temperature ramped to the set point temperature (T_{sp}) in 10 minutes and held at T_{sp} until ignition. Parameters describe tests 103 (T_{sp} = 415.5 K), 104 (T_{sp} = 413.5 K), 105 (T_{sp} = 409.5 K for about 2 hours then ramped at 21.4°C/minute until ignition), 106 (T_{sp} = 405.5 K then ramped to 423.5 after 5 hours), 107 (T_{sp} = 423.5 K), 114 (T_{sp} = 415.5 K), 115 (T_{sp} = 438.7 K), and 116 (T_{sp} = 407.5 K).
[e]detonators encased in copper cylinder with outside temperature exposed to constant temperature ramp or ramp and hold.

EXPERIMENTS

ONE-DIMENSIONAL TIME TO EXPLOSION (ODTX)

The Catalano et al. [16] ODTX experiment is shown in Figure 3 where preheated aluminum anvils were used to confine 1.27 cm diameter spheres of PETN to 1500 atm. Heaters controlled the temperature of the anvils to ±0.2 K, and the primary measurement was the "time to explosion." Figure 3 shows a schematic of the original ODTX apparatus constructed in 1975. The PETN data was obtained in 1987 on a lot of PETN received in 1965 [17]. The aged PETN is assumed to behave similar to fresh PETN used in the SITI experiments described subsequently.

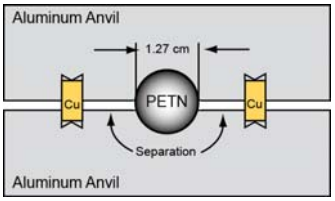

Figure 3. ODTX schematic

SANDIA'S INSTRUMENTED THERMAL IGNITION (SITI) EXPERIMENTS

The SITI experiment [1], shown schematically in Figure 4.A and 4.B, had type K 76 μm diameter thermocouples located at various radial positions in the center of a 2.54 cm diameter by 2.54 cm tall cylinder of PETN. The outside temperature of the confining aluminum cylinders was maintained at a controlled set point using a coil heater. For most of the PETN experiments, the outside temperature of the aluminum confinement was ramped from room temperature to the set point temperature in 10 minutes and held until the PETN ignited. The experiment also has a pressure tap to monitor pressure.

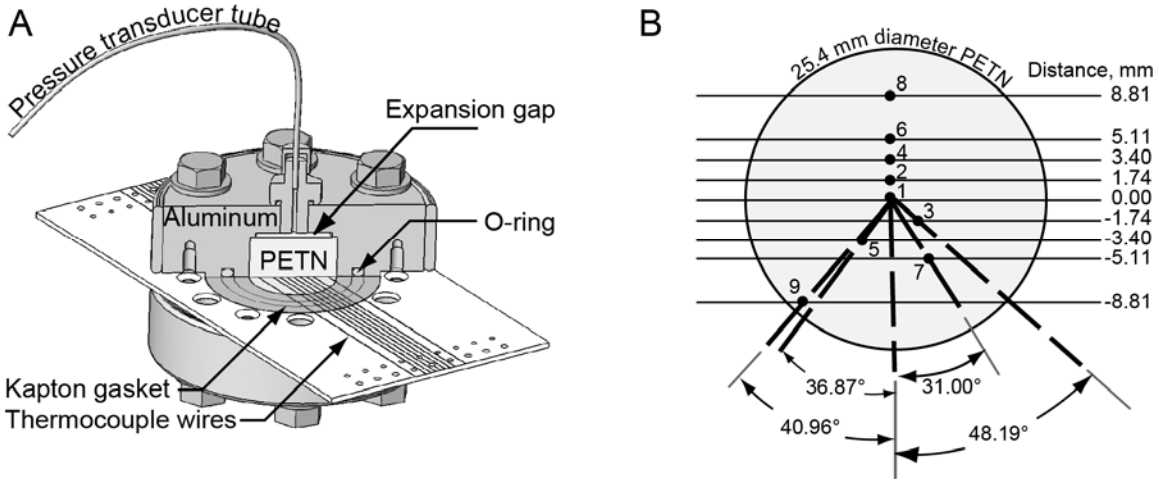

Figure 4. A) Schematic and B) cross section of the SITI experiment.

DETONATOR

A detonator encased in copper is shown schematically in Figure 5. The copper was wrapped in electric heating tape, insulated, and heated between 9 and 20°C/minute [6]. For one test, the boundary was ramped to 153°C and held until ignition. The lead azide does not react until 220°C, which is well above temperatures at which the PETN thermally ignites [6]. Thus, the lead azide was considered nonreactive in the simulations. Typical properties were used for the lead azide, air and rubber.

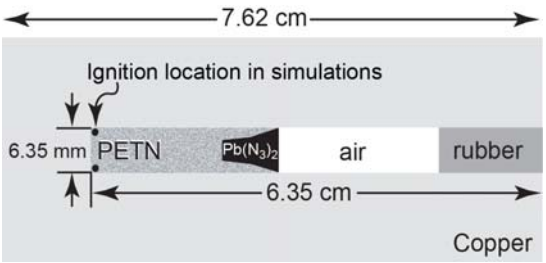

Figure 5. Schematic of detonator in copper cylinder.

SIMULATIONS

MESH AND SOLUTION METHOD

Figure 6 shows 4 meshes corresponding to the experiments described in Table 4—one ODTX mesh, two SITI meshes, and one detonator mesh. The equations listed in Table 1 were solved using a preconditioned conjugate gradient solver with the finite element code Calore [9]. The endotherm associated with melting was included by using the effective thermal capacitance shown in Figure 2. The PETN material parameters were taken from Table 3. Parameters that are specific to each experiment such as density were taken from Table 4.

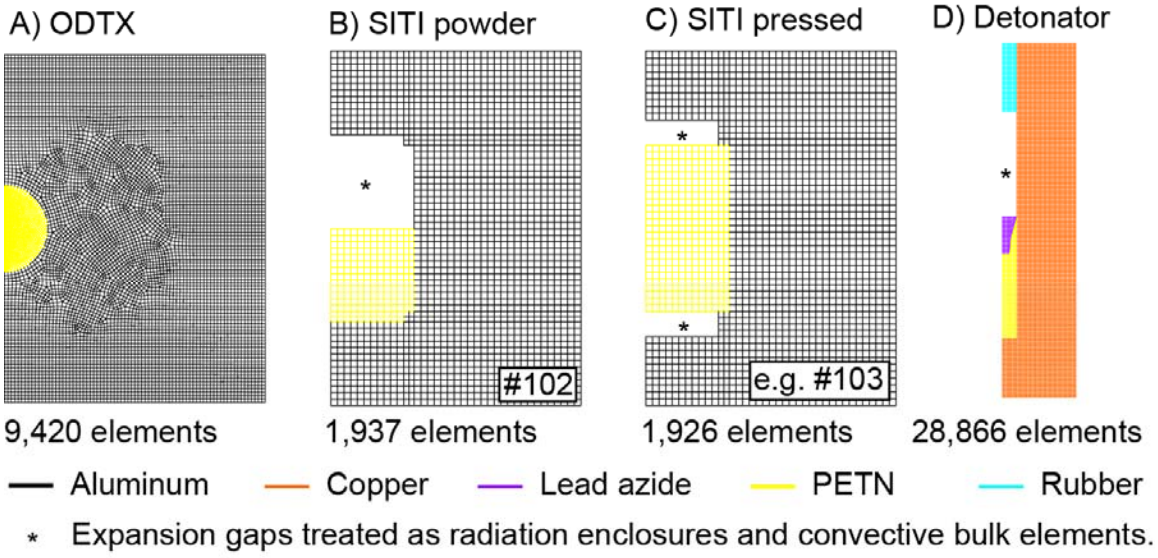

Figure 6. Two dimensional (2D) axisymmetric meshes with quadratic elements for experiments listed in Table 4.

Uncertainties in the calculated results for the ODTX and SITI simulations were determined using a Latin hypercube sampling (LHS) technique. The LHS technique is an efficient, *constrained sampling* technique developed by McKay et al. [18] and is used to propagate uncertainty into the predicted results. Ten parameters—α_c, α_g, C_{eff}, k_L, k_{rate}, k_s, T_{pc}, w_{pc}, ξ, and ρ_{bo}—listed in Tables 3 and 4 were assumed to vary uniformly about their nominal values. Uncertainties in the enclosure volume and tube volume were found to be insignificant in previous work with TNT [19] and were not considered in the current work. In the current work, 2*n* samples were run for each LHS analysis. Thus 20 LHS runs were made for each boundary temperature for the ODTX and SITI simulations. The dispersions in ignition time are presented using the range of the LHS simulations. Examination of scatter plots of the ignition time versus the LHS parameter values were used to judge strongly organized relationships between the model parameters and the model response.

TIME TO IGNITION

Figure 7.A shows the mean and range of the 20 LHS simulations for both the ODTX and SITI simulations for set point temperatures (T_{sp}) ranging from 403 to 500 K. The anvil temperatures were held at T_{sp} giving a constant temperature boundary temperature for the ODTX experiments. The external temperatures were ramped from room temperature to T_{sp} in 10 minutes and held at T_{sp} for the SITI experiments.

Figure 7.B and 7.C shows the scatter in time to ignition for various values of the phase change temperature and liquid rate multiplier, which had the highest linear correlation coefficient between ignition time and the variation in the input value. Clearly, the uncertainty in the phase

change temperature affects the uncertainty when 1000/T is between 2.35 and 2.45. This corresponds to temperatures ranging from 408 to 425 K, where endothermic energy changes occur as shown by the effective capacitance in Figure 2. The uncertainty is associated with the latent enthalpy, but with the reaction rate increasing due to liquefaction. The sensitivity of the ignition time to the liquid rate multiplier is shown in Figure 7.C.

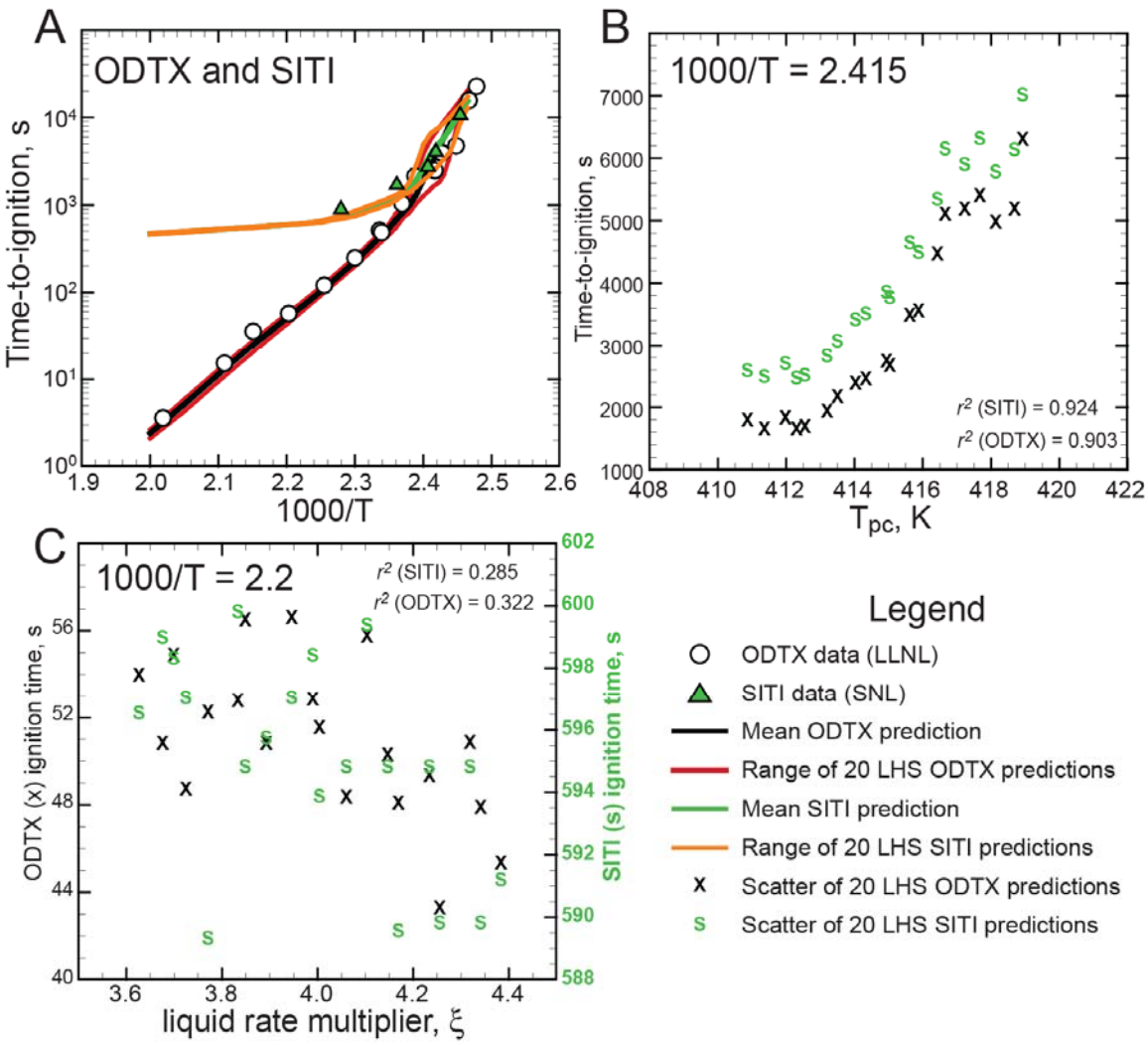

Figure 7. Ignition and selected scatter plots for ODTX and SITI simulations of PETN.

Zucker et al. [6] reported that the detonators heated at 9 and 20°C/min ignited when the temperature reached 168°C and 175.5°C, respectively. Thus, for these two heating rates of 9 and 20°C/min, the detonators ignited after approximately 940 s and 446 s, respectively. The model of the detonators predicted ignition after 950 s and 447 s, respectively. Clearly the prediction of time to ignition is adequate, especially when the boundary temperature is ramped.

Zucker et al. also performed one test in which the boundary temperature was ramped at an unspecified rate to 153°C and held until ignition. Since the heating rate at 100% power was measured at 17.33 and 19°C/min, the average or 18°C/min was used in a simulation of the detonator. In the simulation, the boundary temperature was set to reach 153°C after 423 seconds and then the boundary temperature was held at 153°C. The predicted ignition with this boundary temperature profile occurred at 710 s. Zucker et al. stated that ignition for this ramp and hold experiment occurred after ~700 s.

TEMPERATURE AND PRESSURE

Only the SITI experiments had internal temperature and pressure measurements. Predicted and measured internal temperatures, pressures, and ignition times are shown in Figure 8 for three of the SITI runs—#102, 103, and 105. The PETN melting point range is also shown in Figure 8. Post ignition photos of each of these experiments are also shown in Figure 8. The PETN ignition model adequately simulates the internal temperatures, pressures, and ignition times but does not calculate violence. Post ignition pictures of these SITI experiments are also shown in Figure 8. The responses were classified as a fizzle, nonviolent burst, or violent burst.

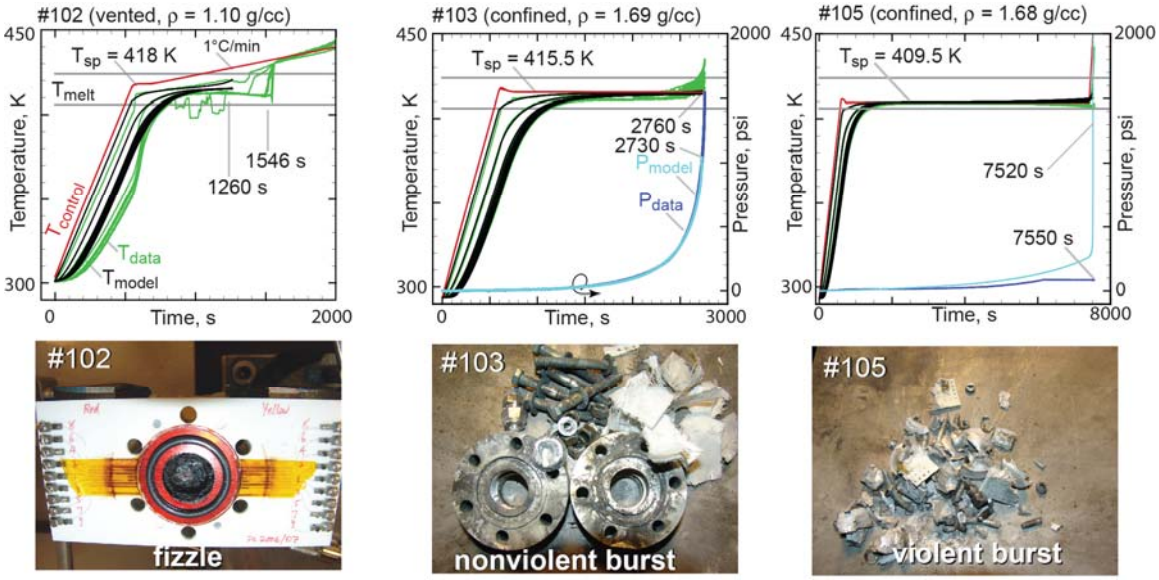

Figure 8. Predicted (black lines) and measured (green lines) internal temperatures at locations specified in Figure 4.B for the SITI runs 102, 103, and 105. The red line is the control temperature. Predicted (cyan lines) and measured (blue lines) pressure for each of these SITI experiments are also shown on each plot. The ignition times are also indicated on each plot. Pictures of the post ignition experiments show the range of violence in the SITI experiments.

CORRELATING COOKOFF VIOLENCE

Violence in detonator experiments was correlated with the maximum expansion of the copper confinement. Zucker et al. [6] detonated the PETN in the copper confinement tube at room temperature with no preheating and found the expansion to be about 7.8 mm. The shapes of the copper confinement after ignition for the ramped experiments were teardrop shaped with the widest part near the bottom [6]. This is in agreement with the predicted location of the ignition shown in Figure 5. The shape of the copper confinement after ignition for the "ramp and hold" experiment had the widest shape near the lead azide charge and was the least violent of all of the experiments. Zucker observed expansions of ~8 mm when the heating rates were greater than 9.53°C/min. For heating rates less than and equal to 9.53°C/min, the cylinders only expanded ~3 mm.

A method was developed to predict the effectiveness of the detonators following ignition by computing dimensionless Damköhler numbers. The Damköhler number has been used traditionally to relate reaction time scales to other phenomena occurring in a system. In the current work, a conductive and storage Damköhler number are defined as follows:

$$D_{a,c} = D_a \mathrm{IV} = \frac{\text{reaction time scale}}{\text{conduction time scale}} = \frac{\rho_b h_r r}{\nabla\cdot(k\nabla T)} = \frac{h_r r}{C_b \frac{\partial T}{\partial t} - h_r r} \tag{11}$$

$$D_{a,s} = \frac{\text{reaction time scale}}{\text{storage time scale}} = \frac{h_r r}{C_b \frac{\partial T}{\partial t}}. \tag{12}$$

The conductive Damköhler number ($D_{a,c}$) is traditionally referred to as the Damköhler Group IV (D_aIV) number [20]. The storage Damköhler number ($D_{a,s}$) is useful to determine when the PETN reactions runaway. The conductive Damköhler number becomes unstable when ignition is approached. However, the storage Damköhler number is smooth up to the ignition point and is a better indicator of the onset of ignition. However, both the conductive and storage Damköhler numbers are unstable for boundary conditions where the boundary temperature is held at a constant set point temperature since temperature gradients are small. Stable solutions, even up to ignition, can be obtained for these cases by setting the temporal temperature gradient to 1 K/s.

Figure 9 shows the calculated reacted gas mass for detonators when the external boundary is ramped between 5 and 20°C/min, and when the external boundary is ramped to 155°C and held until ignition. The symbols represent the time when the maximum storage Damköhler number ($\partial T/\partial t$ = 1 K/s) exceeds 20 giving a consistent prediction of the onset of ignition. The critical mass loss for violence was drawn on Figure 9 to delineate the violent and nonviolent detonator responses. Color contour plots with white limit fringes are also shown in Figure 9 for the most violent and least violent condition--20°C/min ramp and the condition where the boundary is held constant at 155°C. The specific reasons for the differences in violence are not predicted. However, one might speculate reasons for violence from the state of the PETN at the onset of ignition. For example, substantially more liquid formation may have reduced the number of hot spots causing a slower and less violent post ignition burn. Figure 10 shows a similar plot for the SITI simulations. Post ignition pictures of the experiments shown in Figure 10 were used to determine the critical mass loss for these experiments.

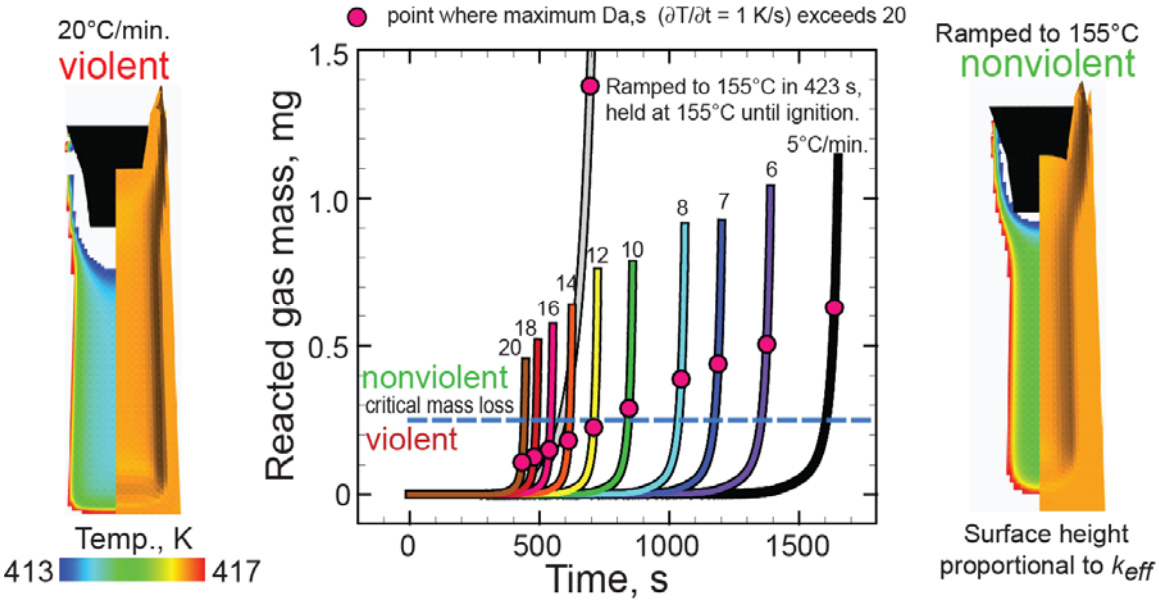

Figure 9. Cookoff violence in Zucker's detonators [6] correlated with the extent of reaction at the onset of ignition.

SUMMARY AND CONCLUSIONS

Decomposition of PETN was modeled with a single-step mechanism using a modified Arrhenius reaction rate. The reaction rate was assumed to be independent of pressure and the activation energy was assumed to be normally distributed with respect to the reaction progress. The decomposition products were assumed to be in chemical equilibrium. The mean activation energy was taken to be the same as the activation energy used by Makashir and Kurian [14]. The reaction rate in the liquid was assumed to be four times the reaction rate in the solid PETN. The melting point was used to transition the rates from solid-phase reaction rates to liquid-phase reaction rates.

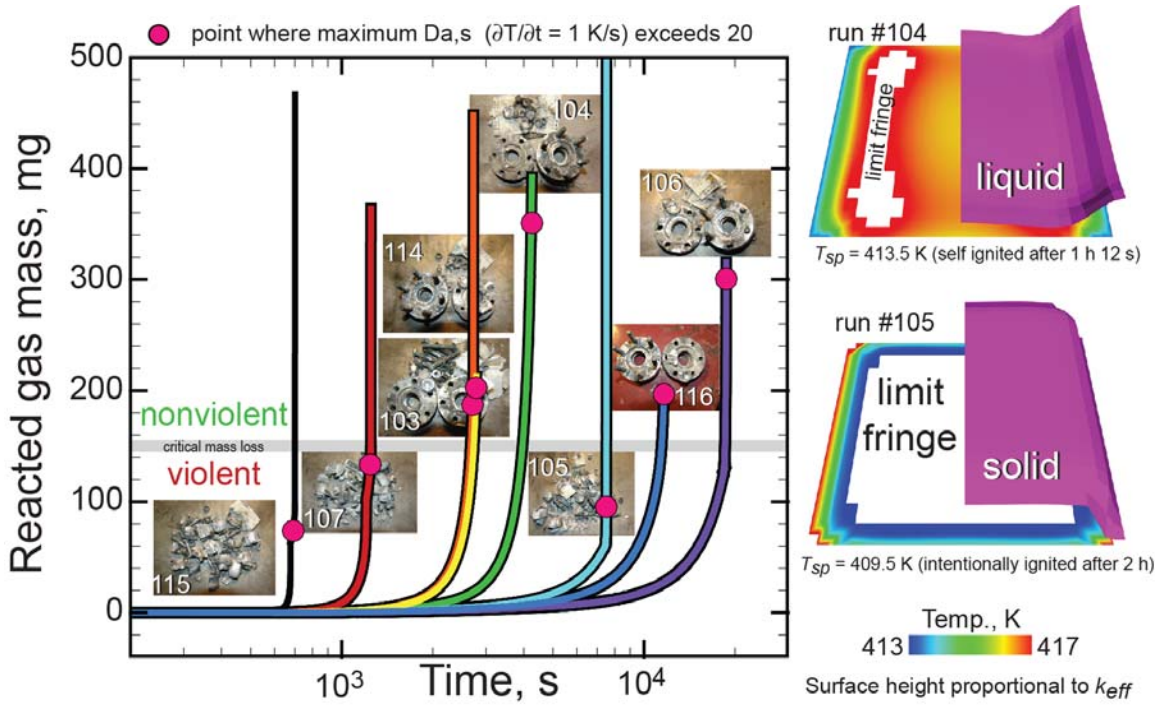

Figure 10. Cookoff violence in SITI experiments correlated with the extent of reaction at the onset of ignition.

Thermal conductivity at temperatures below reaction thresholds were obtained from the SITI experiments. Thermal conductivities at higher temperatures were determined using an effective thermal conductivity model that separates conductive heat transfer into three parts: conduction through the condensed PETN, conduction through the gas decomposition products, and radiation through the decomposing PETN. Evolving gas volume fraction and bulk densities were calculated as field variables. Pressures were determined as an integral quantity by assuming the gas velocities were significantly less than sound speeds. Thus, pressure was assumed to be spatially constant but varies in time as the PETN decomposes.

Uncertainty in the decomposition model was determined using an LHS analysis of both the SITI and ODTX experiments. The parameter that affected the uncertainty in the ignition time the most was the melting point temperature. The melting point temperature was used to transition the reaction rates between solid and liquid reaction rates, which differed by a factor of four.

The PETN model was validated by simulating thermal ignition of a detonator. The data for the detonator and estimate of reaction violence was presented by Zucker et al. [6]. The measured and predicted ignition times were extremely close. For example, the predicted and measured ignition time for the detonator ramped at 20°C/min was 447 and 446 seconds, respectively. The model predicted the time-of-ignition and the location of ignition adequately.

A method was presented to assess whether or not the detonator would function as designed (violent response) after thermal ignition or to function below design (dud). The method was to compare the extent of reaction, at the time that the calculated maximum storage Damköhler number exceeded 20, to a threshold value reacted gas. If the reacted gas mass was below the threshold value at the onset of ignition, the detonator was predicted to have the same metal deforming output as the design mode expansion. If the reacted gas mass was above the threshold value at the onset of ignition, the detonator was predicted to be a dud. A similar analysis was performed on the SITI experiments, which had a different reacted gas threshold.

This simple empirical method may be useful to determine whether or not reactive components that contain PETN would fail to function during abnormal thermal events such as fire or would give the same metal deforming output as an intentionally ignited detonator. The estimate of violence worked well for the detonator described in the current work because the mass was small

and the spatial temperature was fairly uniform. However, the specific reasons for violence were only speculated without experimental evidence. More work is needed to see if this technique could be applied to larger systems.

The PETN model does not predict violence. The PETN model predicts ignition based on thermal runaway. A modified storage Damköhler number with the temporal temperature gradient set to 1 K/s was used as a consistent method to predict the onset of ignition. When the maximum value of the storage Damköhler number exceeded 20, the calculation was near the ignition point. This criterion was shown to be valid for both ramped experiments and isothermal experiments. The state of the PETN at the onset of ignition gives the degraded state of the material that may be used to consistently compare ignition states to help determine if the subsequent burn will be violent or benign. The violence assessments are only valid for a given system. Different PETN mass, volume, and confinement will results in a different violence threshold that should be determined with experimental data.

FUTURE WORK

Mass loss and decomposition gases molecular weight are inferred assuming equilibrium. Measurements are needed to quantify these assumptions. Most PETN cookoff experiments are fully confined. More experiments are needed to assess the affect of pressure and confinement on PETN decomposition. The violence correlation for the SITI experiments should also be done with experiments ramped at different rate as in the detonator simulations to see if the predicted violence threshold of 150 mg of reacted gas holds true for different heating conditions.

ACKNOWLEDGMENTS

Work was performed at Sandia National Laboratories (SNL). Sandia is a multiprogram laboratory operated by Sandia Corporation, a Lockheed Martin Company, for the United States Department of Energy's National Nuclear Security Administration under Contract DE-AC04-94AL85000. I would like to thank Mel Baer for suggesting using Damköhler numbers to evaluate reaction violence; Craig Tarver and Tri Tran at Lawrence Livermore National Laboratory for supplying the ODTX data; Bob Patton (SNL) for the DSC data; Bill Erikson and Dean Dobranich for reviewing the document; and Terry Aselage and Imane Khalil (SNL) for management support.

REFERENCES

1. Kaneshige, M. J.; Renlund, A. M.; Schmitt, R. G.; and Erikson, W. W.; "Cook-off Experiments for Model Validation at Sandia National Laboratories," *Twelfth International Detonation Symposium*, Office of Naval Research ONR 333-05-2, San Diego, CA, 821 (2002).
2. Tarver, C.M.; Tran, T.D.; and Whipple, R.E.; "Thermal Decomposition of Pentaerythritol Tetranitrate," *Propellants, Explosives, Pyrotechnics*, **28** (4), 189 (2003).
3. Zinn, J. and Mader, C.L.; "Thermal Initiation of Explosives," *J. Appl. Phys*., **31**(2), 323 (1960).
4. Zinn, J. and Rogers, R.N.; "Thermal Initiation of Explosives," *J. Phys. Chem*., **66** (12), 2646 (1962).
5. Merzhanov, A.G. and Abramov, V.G.; "Thermal Explosion of Explosives and Propellants. A Review," Propellants, Explosives, Pyrotechnics, **6** (5), 130 (1981).
6. Zucker, J.M.; Dickson, P.; and Sanders, V.E.; "Thermal Initiation of Non-Electric Detonators," *Propellants, Explosives, Pyrotechnics*, **34** (2), 142 (2009).
7. Hobbs, M. L.; Wente, W.B.; and Kaneshige, M. J.; "Modeling PETN Ignition," to be submitted to *J. Phys. Chem. A.* (2009).
8. Hobbs, M. L.; Baer, M. R.; and McGee, B. C.; "JCZS: An Intermolecular Potential Database for Performing Accurate Detonation and Expansion Calculations," *Propellants, Explosives, Pyrotechnics*, **24** (5), 269 (1999).
9. Bova, S. W.; Copps, K. D.; and Newman, C. K.; "Calore—A Computational heat Transfer Program," Sandia National Laboratories Report SAND2006-6083P, Albuquerque, NM (2006).

10. Manelis, G.B.; Nazin, G.M.; Rubtsov, Y.I.; and Strunin, V.A., *Thermal Decomposition and Combustion of Explosives and Propellants*, Taylor & Francis, New York (2003).
11. Gibson, L. J. and Ashby, M. F.; *Cellular solids Structure and properties—Second edition*, Cambridge University Press, Cambridge, UK, (1997).
12. Siegel R. and Howell, J. R. *Thermal Radiation Heat Transfer—Third Edition*, Taylor & Francis, Washington DC (1992).
13. Gibbs, T.R. and Popolato, A.; Editors, LASL Explosive Property Data, University of California Press, Los Angeles, CA, 134 (1980).
14. Makashir, P.S. and Kurian, E.M.; "Spectroscopic and Thermal Studies on Pentaerythritol Tetranitrate (PETN)," *Propellants, Explosives, Pyrotechnics*, **24**, 260 (1999).
15. Incropera F. P. and DeWitt, D. P.; *Fundamentals of Heat and Mass Transfer*, Fifth Edition, John Wiley & Sons, New York (2002).
16. Catalano, E.; McGuire, R.; Lee, E.; Wrenn, E.; Ornellas, D.; Walton, J.; "The Thermal Decomposition and Reaction of Confined Explosives," *Sixth Symposium (International) on Detonation*, Office of Naval Research ONR ACR-221, Coronado, CA, 214 (1976).
17. Tran, T.D., Lawrence Livermore National Laboratory, private communication (2008).
18. McKay, M. D.; Conover, W. J.; and Beckman, R. J.; "A Comparison of Three Methods for Selecting Values of Input variables in the Analysis of Output from a Computer Code," *Technometrics*, **21** (2), 239 (1979).
19. Hobbs, M.L.; Kaneshige, M.J.; Gilbert, D.W.; Marley S.K.; and Todd, S.N.; "Modeling TNT Ignition," *J. Phys. Chem. A*, , **113** (39), 10474 (2009).
20. Catchpole, J.P. and Fulford, G.; "Dimensionless Groups," *Industrial and Engineering Chemistry*, **58** (3), 48 (1966)